

Low-frequency spectra of nearby galaxies with LOFAR

Krzysztof T. Chyży¹, Wojciech Jurusik¹,
Julia Piotrowska¹ and Małgorzata Curyło¹

1. Astronomical Observatory of the Jagiellonian University, Orla 171, 30–244 Kraków, Poland

We explored low-frequency spectra of galaxies in a sample of objects of the Local Universe. From estimated 150 MHz fluxes from the LOFAR Multifrequency Snapshot Sky Survey (MSSS) and fluxes at various frequencies obtained from the literature search we constructed integrated radio spectra of the sample of galaxies and looked for spectral flattenings and turnovers. We modelled thermal (free-free) absorption and deviations from a simple power-law synchrotron spectra and looked for evidences of cool ionized gas in these galaxies. Finally, we discussed how incoming LOFAR surveys will enable investigation of more distant universe and we put predictions on the shape of radio spectra of high-redshift galaxies.

1 Introduction

So far, radio studies of galaxies have been conducted in a systematic way mainly at frequencies above 300 MHz. Problems with signal calibration due to high influence of the Earth ionosphere at low frequencies did not allow for the construction of instruments of high spatial resolution and sensitivity. LOw Frequency ARray (LOFAR) is a modern phased-array radio interferometer designed to overcome these problems (van Haarlem et al., 2013). It consists of 51 stations spread across Europe, including three single stations located in Poland, and covers frequency range between 10 - 240 MHz. The innovative digital system along with very long baselines makes LOFAR an excellent tool for studying radio sources at the highest sensitivity, spatial and spectral resolution achieved so far in this frequency regime (van Haarlem et al., 2013).

Previous attempts to investigate galaxy spectra at low frequencies showed that various physical processes can influence their shape (Lacki, 2013). Israel & Mahoney (1990, hereafter IM) compared observed galaxy flux densities at 57.5 MHz with values extrapolated from higher frequencies. They have concluded that these spectra are flatter at low frequencies and that this flattening is increasing function of the galaxy viewing angle. Such phenomenon could be explained by increasing thermal absorption of synchrotron emission with increasing galaxy tilt. A special phase of the interstellar medium (ISM) of ionized but relatively cool ($T < 1000$ K) gas was proposed to explain this absorption. However, other authors came to different conclusions: e.g. Hummel (1991) reanalysed the same data, confirmed reduction of radio emission but questioned the dependence of the spectral flattening on galaxy inclination. The author suggested changes in high-frequency spectra due to energy losses of cosmic ray electrons (CREs) when propagating across the galaxy.

Until now there are only a few studies exploring properties of galaxies based on LOFAR data. One of them is a detailed investigation of M51 galaxy which shows

that the arm-interarm radio emission contrast is lower at 151 MHz than at 1400 MHz (Mulcahy et al., 2014). This was interpreted as propagation of CREs from spiral arms into interarm regions. It was also shown that the integrated spectrum of M51 follows a simple power-law but in the central region the local spectrum flattens due to thermal absorption.

Subarcsecond resolution observations of M82 starburst galaxy at 118 MHz and 154 MHz were performed with LOFAR using international stations (Varenius et al., 2015). As a result, the authors reported detection of 16 compact objects, including seven that were not previously catalogued. They also indicated absorption effects along the central part of the star-forming disk and the strongest one towards the centre of M82.

In this article we present preliminary investigation of low-frequency spectra of nearby galaxies based on LOFAR observations and literature data. We build a 3D model of galaxy radio emission to analyse and interpret the actual spectra of M51 and M82 galaxies and assess the role of thermal absorption in shaping galaxy spectra. A more systematic studies of a larger sample of galaxies are in preparation.

2 Observed galaxy spectra

We constructed a sample of nearby galaxies based on compilation of IRAS Redshift Survey sources having radio counterparts in the NRAO VLA Sky Survey at 1.4 GHz (Yun et al., 2001). Selection of chosen galaxies was based on the following criteria:

- the galaxies are of spiral or irregular Hubble Type ($T \geq 0$),
- they have radio flux density $S > 50$ mJy at 1.4 GHz,
- they are visible at the northern hemisphere,
- they show no significant emission from an active galactic nuclei (AGN).

We obtained 200 objects fulfilling these criteria. In this preliminary study we restricted the sample to 34 galaxies suitable for further analysis. For these sources we constructed the integrated (global) galaxy spectra based on the flux measurements from the LOFAR Multifrequency Snapshot Sky Survey (MSSS) at 150 MHz (Heald et al., 2015) and from published flux densities at other frequencies. We present two examples of such galaxy spectra in Fig. 1. The spectra show only weak curvatures indicating small flattenings and no turnovers at low frequencies.

IM have found that the observed fluxes at 57.5 MHz are systematically smaller than those extrapolated from higher frequencies and our sample confirms this trend. Contrary to IM, who has explained this tendency as increasing thermal absorption with growing inclination, we found no relation between low-frequency spectral flattening versus galaxy tilt. Therefore, the low-frequency flattening must be caused by other effects and we do not see the need for low-temperature ionised gas postulated by IM. However, thermal absorption seems to be the only proper explanation of the radio emission drop in the centre of M82 at 150 MHz (Varenius et al., 2015) and in other galaxies. In order to interpret all these results we performed a 3D numerical model of radio emission of galaxies of different star-forming activity to allow analysis of thermal absorption and projection effects.

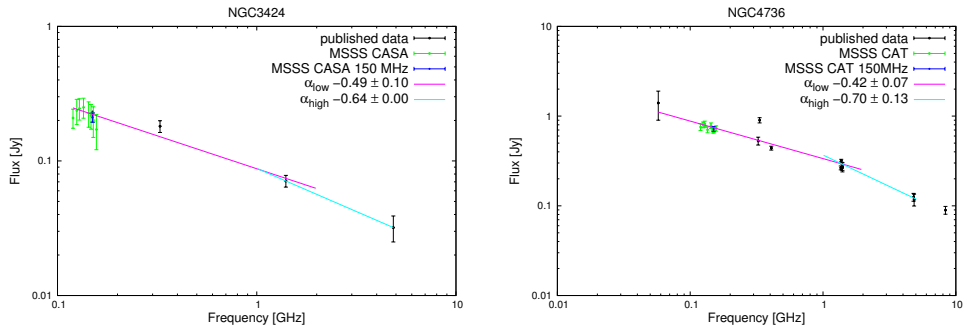


Fig. 1: The results of radio spectra for individual galaxies: NGC 3424 (left) and NGC 4736 (right). The black dots represent published data, the green dots represent the MSSS data in eight individual bands, the blue dot represents the interpolated MSSS flux density at 150 MHz, the magenta and cyan lines show the fitted low- and high-frequency power-law spectra, respectively.

3 Thermal absorption

In our numerical model we take into account several galaxy building blocks like the core, thin and thick disks. In the model grid we set parameters describing thermal emission and absorption, as well as synchrotron emission which reflects cooling of CREs and distribution of the magnetic field. Then we solve the radiative transfer equation along the line of sight at different frequencies and for different galaxy viewing angles. We distinguish two solutions of the radiative transfer in the cell n depending on the content of the current and preceding cells:

$$S_n = \begin{cases} S_{n-1} e^{-\tau_n} + (2kT_e \nu^2 c^{-2} + B_n \tau_n^{-1}) (1 - e^{-\tau_n}) \Omega \\ S_{n-1} + B_n \Omega \end{cases} \quad (1)$$

where

$$\tau_n = 8.235 \times 10^{-2} \left(\frac{T_e}{\text{K}} \right)^{-1.35} \left(\frac{\nu}{\text{GHz}} \right)^{-2.1} \left(\frac{EM_n}{\text{pc cm}^{-6}} \right) \quad (2)$$

is the optical thickness of thermal gas in a cell of size s , T_e is the thermal electron temperature, EM_n is the emission measure, B_n is the synchrotron intensity in the cell n and Ω is the solid angle of this cell.

The first solution of Eq. (1) corresponds to the cell filled with mixed synchrotron and thermally emitting gas. Radio emission from the previous cell in the line of sight (S_{n-1}) is absorbed by thermal gas in the cell number n . The second solution of Eq. (1) applies to the cell with only synchrotron emission which can be seen in e.g. galaxy halo. By solving the radiative transfer equation for all cells in the grid for a particular viewing angle and at different frequencies, we obtained the synthetic maps of radio emission at various frequencies. We then integrated the flux density from these maps and constructed the modelled galaxy spectra for selected inclination angles.

We modelled two individual galaxies: M51 – an almost face-on galaxy with relatively low star formation rate, and M82 – a starburst galaxy, seen almost edge-

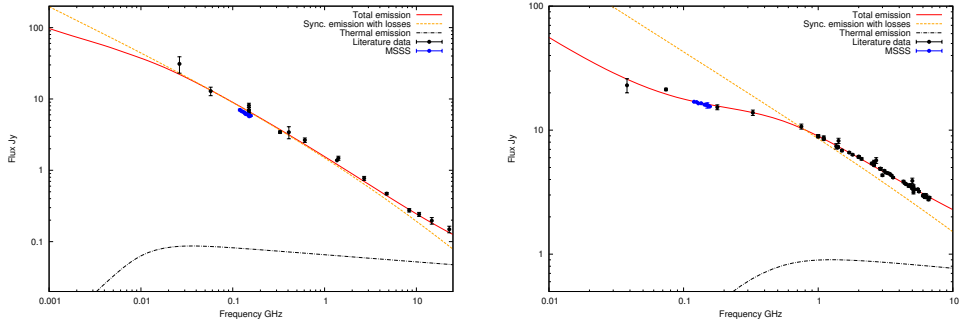


Fig. 2: Results from our 3D modelling: the global spectra (in red) for M51 (left) and for M82 (right), the synchrotron components without absorption (orange dotted line), and the component of the thermal gas (black dashed line). The points show the observational data.

on. For both objects detailed informations about distribution of thermal and non-thermal radio emissions are available in the literature. Modelled spectra are well matched to observational data (Fig. 2) and M82 shows stronger depression in emission due to thermal absorption.

4 Discussion and summary

Our analysis of the spectra of the sample galaxies indicate that they are slightly flatter at low frequencies which seems to confirm similar result by IM. However, our studies do not show any correlation of these spectral features with galaxy tilt and therefore cannot be explained by thermal absorption. We suggest that such spectral curvatures can arise from energy losses of CREs when interacting with synchrotron and inverse Compton radiation at high frequencies. Similar conclusion was drawn by Marvil et al. (2015).

In order to explain shapes of integrated low-frequency spectra of nearby galaxies we constructed a 3D model of galaxy emission. Our modelling of M51-like galaxy suggests the following:

- Thermal absorption effects can be seen only in model radio maps at frequencies below ≈ 30 MHz and in global spectrum at frequencies as low as 20 MHz (Fig. 2, left panel). The weak flattening observed in some galaxy spectra of our sample above this frequency can arise from the curvature of the synchrotron spectrum.
- The modelled local spectra of the central regions of galaxies show significantly curved spectra and even turnovers for edge-on galaxies at frequencies of about 100-200 MHz. High-resolution observations at low frequencies (as reported in Sect. 1) are essential for their detection.

The models of M82-like galaxies give the following results:

- As compared to M51 the models of M82 show much stronger absorption effects (Fig. 2, right panel).

- The modelled local spectra of starburst galaxies seen at various viewing angles reveal strong turnovers at high frequencies at about 1 GHz for the galaxies visible edge-on and at about 500 MHz for the face-ons. Therefore, we predict much stronger free-free absorption effects and significant changes in the radio spectra of luminous infrared galaxies and more distant galaxies with high star formation rate. Since starburst galaxies are not frequent in the Local Universe we observe mostly just weak spectral curvatures in our present sample.

Future LOFAR observations of deep fields will probe more distant galaxies. The incoming more sensitive LOFAR surveys (Shimwell et al., 2017) and especially those from the low band antenna (≈ 50 MHz) are highly needed to distinguish between different processes causing spectral curvatures of highly star-forming galaxies in more distant universe and understand the variations in spectral curvature during the galaxy evolution.

Acknowledgements. We thank for the help of the Academic Computer Centre CYFRONET AGH in Krakow, Poland, where our numerical analysis were partly performed with the use of the computing cluster Prometheus. WJ acknowledges the support by the Polish National Science Centre grant No. 2013/09/N/ST9/02511. This paper is based (in part) on data obtained with the International LOFAR Telescope (ILT). LOFAR (van Haarlem et al., 2013) is the Low Frequency Array designed and constructed by ASTRON. It has facilities in several countries, that are owned by various parties (each with their own funding sources), and that are collectively operated by the ILT foundation under a joint scientific policy.

References

- van Haarlem, M. P., Wise, M. W., Gunst, A. W., et al., *A&A* **556**, A2 (2013)
- Heald, G., Pizzo, R. F., Orrú, E., et al., *A&A* **582**, A123 (2015)
- Hummel, E., *A&A* **251**, 442 (1991)
- Israel, F. P., Mahoney, M. J., *ApJ* **352**, 30 (1990)
- Lacki, B. C., *MNRAS* **431**, 3003 (2013)
- Marvil, J., Owen, F., Eilek, J., *ApJ* **149**, 32 (2015)
- Mulcahy, D., Horneffer, A., Beck, R., et al., *A&A* **568**, A74 (2014)
- Shimwell, T. W., Röttgering, H. J. A., Best, P. N., et al., *A&A* **598**, A104 (2017)
- Varenius, E., Conway, J. E., Martí-Vidal, I., et al., *A&A* **574**, A114 (2015)
- Yun, M., Reddy Naveen, A., Condon, J. J., *ApJ* **554**, 803 (2001)